Deconvolution-based resolution enhancement of chemical ice core records obtained by continuous flow analysis

Rasmussen, Sune Olander; Andersen, Katrine K.; Johnsen, Sigfus Johann; Bigler, Matthias; McCormack, T.

Deconvolution-based resolution enhancement of chemical ice core records obtained by Continuous Flow Analysis

S. O. Rasmussen[1], K. K. Andersen[1], S. J. Johnsen[1], M. Bigler[1,2], and T. McCormack[3]

Abstract. Continuous Flow Analysis (CFA) has become a popular measuring technique for obtaining high-resolution chemical ice core records due to an attractive combination of measuring speed and resolution. However, when analyzing the deeper sections of ice cores or cores from low-accumulation areas, there is still need for further improvement of the resolution. Here a method for resolution enhancement of CFA data is presented. It is demonstrated that it is possible to improve the resolution of CFA data by restoring some of the detail that was lost in the measuring process, thus improving the usefulness of the data for high-resolution studies such as annual layer counting. The presented method uses deconvolution techniques and is robust to the presence of noise in the measurements. If integrated into the data processing, it requires no additional data collection. The method is applied to selected ice core data sequences from Greenland and Antarctica, and the results demonstrate that the data quality can be significantly improved.

1. Introduction

Chemical ice core records contain a wealth of information about the composition of the past atmosphere and provide information about large-scale changes of circulation patterns and climatic conditions in both the source regions and on the polar ice sheets [Legrand and Mayewski, 1997]. If the depth resolution of the measurement is sufficient even annual layers and events on a sub-annual time scale can be resolved. Examples include deposits from volcanic eruptions [e.g. Bigler et al., 2002], biomass burning events [e.g. Fuhrer et al., 1996], and the identification and counting of annual layers, which is of paramount importance for the precise dating of ice cores [Hammer et al., 1978; Meese et al., 1997; Alley et al., 1997].

In recent years, the use of Continuous Flow Analysis (CFA) systems has become increasingly popular for chemical ice core analysis [Sigg et al., 1994; Anklin et al., 1998; Röthlisberger et al., 2000; McConnell et al. 2002]. Continuously melted subsections of the ice core provide a steady sample flow which is immediately analyzed by means of fluorescence and absorption spectrophotometric detection methods. CFA stands out because good resolution, high measuring speed, and the elimination of time-consuming sample cleaning is combined, without compromising analytical accuracy [Littot et al., 2002]. However, because many meters of ice core have to be analyzed in order to provide long, continuous data sets the trade-off between measuring speed and resolution is still an important issue. The resolution is mainly limited by the geometry of the melting device and by how much turbulent mixing takes place in small volumes within the setup (inside e.g. the debubbler, pump tubes, reaction columns, and flow cells). Although cycles with short wavelengths are obliterated by this mixing some of the lost details can be restored using deconvolution techniques. In this paper a method of restoring CFA data to optimize their potential for example for annual layer counting is presented. The method is mathematically similar to the method used for correcting the effect of the diffusion in the ice of the stable isotopes [Johnsen, 1977; Johnsen et al., 2000]. However, the information needed to correct for diffusion of stable isotopes has to be obtained from diffusion and firnification models whereas in this study the correction can be derived directly from calibration measurements. The method can be integrated in the data processing work line so that only a little extra work is needed. How much the resolution can be improved depends on the signal-to-noise ratio, and at the same time the resolution enhanced data series are filtered in an optimal manner. Although the method is applied only to CFA chemistry data here, it can be used for any liquid-based continuous measurement or sampling system where the sample undergoes mixing before or during the measurement.

2. Data

Two data sources have been used in this work. The method has been developed using data from the North Greenland Ice Core Project (NGRIP) ice core [NGRIP members, 2004], and the method has also been applied to data from the upper part of the ice core from Berkner Island, inside the Filchner-Ronne Ice Shelf, Antarctica, to illustrate that the method is generally applicable and robust.

During the NGRIP field season in year 2000, measurements were performed on the NGRIP deep ice core using a Continuous Flow Analysis (CFA) setup [Röthlisberger et al., 2000]. For the depth interval from 1404.7 to 2930.4 m a 3 cm × 3 cm cross section of ice was cut from the main core in 1.65

[1]Department of Geophysics, University of Copenhagen, Denmark.

[2]Climate and Environmental Physics, Physics Institute, University of Bern, Switzerland.

[3]British Antarctic Survey, Cambridge, United Kingdom.

m pieces and continuously melted for CFA measurements at a speed of $3 - 4$ cm min^{-1}. The analysis systems measured, among other parameters, the concentrations of NH_4^+, Ca^{2+}, NO_3^-, Na^+, and SO_4^{2-} and the electrolytical conductivity of the meltwater [Bigler, 2004]. Although the data collection resolution is around one millimeter, only the actual data resolution only allows identification of cycles with wavelengths down to between one and two centimeters. The presented resolution enhancement method is applied to the NGRIP $[NH_4^+]$, $[Ca^{2+}]$, and conductivity data series only, but could be applied in a similar way to the other NGRIP CFA data series. The resolution enhanced data series from NGRIP are currently being used for interpretation of the NGRIP chemistry record for dating purposes [Rasmussen et al., submitted].

The CFA setup at the British Antarctic Survey used to analyze ice cores from Berkner Island is in principle similar to the NGRIP setup although fewer parameters are measured. Due to the low impurity content in the Holocene part of the ice core, and the fact that Antarctic ice cores in general contain less impurities than Greenland ice cores, the signal-to-noise ratio is significantly worse than for the NGRIP data, especially for the Ca^{2+} subsystem. The resolution enhancement method is applied to a one meter long section of Berkner Island $[Ca^{2+}]$ data from 27 m depth in order to demonstrate how the method deals with noisy data. It should be pointed out that the quality of the presented data section is not representative of the general Berkner Island data quality. The processing of the first season of Berkner Island data is ongoing, for which reason the data are presented in uncalibrated units and on a measurement time scale rather than on a depth scale.

3. Resolution Enhancement

The sample flow from the melting device passes through a debubbler and is split up to feed the different CFA analysis subsystems where it is continuously mixed with reagents that allow fluorescent or absorbent complexes to form. The amount of complex is measured with spectrophotometric detectors, producing a voltage signal which is related to the concentration of the relevant species. In order to convert the voltage signal to concentration, ultra-pure water (blank) is passed through the system before and after the sample to establish the baseline, and standard solutions are measured at regular intervals. The flow of sample, standard solution and blank is illustrated in Figure 1. When the valves switch for example from blank to standard the measured voltage rises from the baseline level and approaches a stable level. This level is used to determine the calibration curve. However, the shape and steepness of the measured curve contains additional information about the nature of the mixing and the relevant time constants in the subsystem. For the Ca^{2+}, NH_4^+, and conductivity subsystems in the NGRIP setup, blank-standard and standard-blank responses are used to estimate the strength of the mixing. The blank-standard and standard-blank response curves must be converted from voltage to concentration before they are used in the analysis. This conversion is straightforward for the NH_4^+ and Ca^{2+} subsystems because the measured voltage from the photomultiplier is linearly related to the concentration. The same holds for the conductivity series which is a direct measurement. This is the reason why these three data series were chosen for the pilot study.

It should be noted that the restoration of the signals presented here is based on response curves obtained from standard measurements. Only the mixing that takes place in the analysis system (the shaded area in Figure 1) is considered while the mixing of the sample that takes place in the melting system and the debubbler unit is excluded. In order to estimate the total mixing, the system's response to blank-standard and standard-blank shifts could be measured by melting a block of clean ice followed by a block of ice with uniform (nonzero) concentration. However, in practice this procedure is not readily performed. Firstly, obtaining ice with evenly distributed impurities is not trivial. Such ice is not available from natural sources, and freezing a standard solution will not produce ice with uniform concentration. Secondly, the ice should have a clean air content similar to that of glacier ice so that the sample-to-air ratio in the segmented flow from the melting device to the debubbler unit is representative of the real measurement conditions. For these reasons, measurements of the total system's response were only carried out by pouring liquid standard and blank solutions directly onto the melting device, but as the conditions were not representative of the real measurement conditions, they have not been used for the resolution enhancement. Consequently only the mixing in the analysis subsystem will be considered. This means that the restoration performed here only accounts for a part of the total mixing, and that additional details possibly could have been restored if good estimates of the total mixing strength had been available.

4. Restoration Filter Design

Restoration of details lost due to mixing can be efficiently handled by deconvolution techniques, operating in either the time domain or the spectral domain. A time-domain approach was tested by Sigg [1990] in order to improve the resolution of CFA $[H_2O_2]$ measurements. The resolution enhancement method presented here is a spectral method where the problem of performing the restoration becomes a question of determining the effect of the mixing as a spectral filter. The spectral approach has the important advantage that it allows a consistent treatment of the noise. The rest of this section is a description of how the filters are constructed from data and calibration measurements. A less mathematical oriented summary can be found as the caption of Figure 2 where the deconvolution filters and the results of the resolution enhanced NGRIP data are exemplified.

Assume that the valves switch at $t = 0$. The incoming, unmixed signal $S(t)$ can then be represented by a step function going from one constant concentration to another. Without loss of generality, the situation can be scaled so that the initial level is zero and that the final level is unity. The incoming signal can thus be represented by the Heaviside function

$$S(t) = \begin{cases} 0 & t < 0 \\ 1 & t \geq 0 \end{cases} \quad (1)$$

but the measured system response to $S(t)$ will be a smooth curve $s(t)$ because mixing has blurred the sharp shift in concentration. In a convolution formulation this corresponds to convolution of $S(t)$ with a mixing response function $M(\tau)$

$$s(t) = \int_{-\infty}^{\infty} S(\tau) \cdot M(t - \tau) d\tau \quad (2)$$

In the spectral domain, convolution is merely multiplication, so the mixing is described by

$$\widetilde{s} = \widetilde{S} \cdot \widetilde{M} \quad (3)$$

where the tilde denotes Fourier transformation. When differentiating equation (2) with respect to time the mixing filter $M(\tau)$ is unaffected and equation (3) becomes

$$\widetilde{s'} = \widetilde{S'} \cdot \widetilde{M} = \widetilde{M} \quad (4)$$

where the last equality comes from the fact that the derivative of a Heaviside step function is the delta function, and that the Fourier transform of the delta function is unity. Thus, the mixing filter $\widetilde{M}$ can be determined by measuring the system response to a step function, differentiating, and performing a Fourier transformation.

During a measuring campaign, the characteristics of the mixing will change. When for example tubes or columns in the setup are changed then the mixing filter will change as well. The mixing filter for the NGRIP NH_4^+ subsystem at the depth 1622 m is shown in Figure 2b (brown curve) as an example. It is seen that the very long wavelengths ($\lambda > 100$ mm) are hardly affected, while the amplitude of a cycle with $\lambda = 10$ mm will be reduced to about 10^{-2} of its original amplitude.

The effect of the mixing can also be illustrated by looking at $s'(t)$ in the time domain. Because s' is the measured response to S', which is a pulse of "delta function shape", s' is called the pulse response. The pulse responses of the three analysis subsystems are illustrated in Figure 3. The curves have been shifted to remove the different time lags introduced by the CFA subsystems, and thus only the shape of the curves should be considered. It is apparent from the width of the curves that the mixing in the conductivity measurement subsystem is much weaker than the mixing in the NH_4^+ and Ca^{2+} subsystems. In the latter, an infinitely sharp pulse is spread out to become an approx. 20 mm wide peak, while the peak produced by the conductivity subsystem is only roughly half as wide. The difference is expected because the conductivity measurement system contains less tubing and no mixing or reaction coils. Because the conductivity measurement subsystem does not contain large mixing volumes, the mixing inferred from the conductivity pulse response can also be regarded as an estimate of the maximum mixing taking place in the melting and debubbling part of the system.

When sample is passed through the analysis system the mixing processes are unchanged. Let D be the unmixed signal entering the analysis system, and d the measured signal. In analogy with equation (3), the original and measured signals are related by

$$\widetilde{d} = \widetilde{D} \cdot \widetilde{M} \qquad (5)$$

where $\widetilde{M}$ is the same filter as in equation (4). Once the mixing filter $\widetilde{M}$ has been determined using the procedure described above the unmixed signal D can then in theory be restored by inverse Fourier transform of $\widetilde{D}$, where

$$\widetilde{D} = \widetilde{d} \cdot \widetilde{M}^{-1} \qquad (6)$$

Cycles with short wavelengths are almost entirely obliterated by the mixing and when the signal is restored using equation (6) the amplitudes of these cycles are consequently heavily amplified. In the presence of noise on the measurements, heavily amplified high-frequency noise will dominate the restored signal. Handling this problem by removing the short wavelengths will in turn remove some of the signal and may cause ringing effects. The optimal trade-off between retaining as much signal as possible without amplifying the noise too much is accomplished by constructing an optimum filter $\widetilde{F}$, or Wiener filter, which for each wave number k is defined as :

$$\widetilde{F}(k) = \frac{P_{signal}}{P_{signal} + P_{noise}} \qquad (7)$$

where P denotes the spectral power of the measured signal and noise, respectively, [Johnsen, 1977]. Determining P_{signal} and P_{noise} is in general not straightforward, but in this work, P_{signal} and P_{noise} are estimated from the spectral power of the measurements $P_{measured}$ as illustrated in Figure 2a. Each of the light green lines (P_{signal} and P_{noise}) is determined as a least squares fit to $P_{measured}$ (orange curve) above and below a certain noise-signal cut-off wavelength (dotted light green line), respectively. The best value of the noise-signal cut-off wavelength is determined by minimizing the total RMS difference between the sum $P_{signal} + P_{noise}$ (dashed green line) and $P_{measured}$ (orange curve) and is 11.6 mm in the presented example. The two light green lines represent the best estimates of the signal and noise parts of the spectral power and $\widetilde{F}(k)$ is calculated according to equation (7) from these estimates (Figure 2b, light green line). In this example, the filter amplitude is close to unity for wavelengths down to 15 mm, while the noise spectral power is about 4 orders of magnitude larger than the remaining signal power for the $\lambda = 6$ mm oscillations.

The optimum filter $\widetilde{F}$ is multiplied with the inverse of the mixing filter $\widetilde{M}^{-1}$ to form the restoration filter $\widetilde{R}$ (Figure 2b, magenta curve), which is used to calculate the best possible estimate of the original data, D_{est} :

$$\widetilde{D_{est}} = \widetilde{d} \cdot \widetilde{F} \cdot \widetilde{M}^{-1} \equiv \widetilde{d} \cdot \widetilde{R} \qquad (8)$$

The restored signal D_{est} can now be determined by inverse Fourier transformation of $\widetilde{D_{est}}$. Alternatively, the restoration filter $\widetilde{R}$ can be transformed back to a time-domain filter $R(\tau)$, which is then used to determine D_{est} from

$$D_{est}(t) = \int_{-\infty}^{\infty} d(\tau) \cdot R(t - \tau) d\tau \qquad (9)$$

without the need of Fourier transforming the data.

5. Results and Discussion

Examples of original (thick lines) and restored (thin lines) NGRIP data are shown in Figure 2c. The selected data section comes from a depth of 1622 m corresponding to the Oldest Dryas (age about 15 ka). From the preliminary NGRIP model time scale [NGRIP members, 2004] the mean annual layer thickness is expected to be about 2 cm. The P_{signal} and P_{noise} curves intersect at $\lambda \approx 11$ mm, suggesting that an annual layer with thickness 11 mm or less will be so heavily weakened by the mixing that it is indistinguishable from the noise. By applying the restoration filter (2b, magenta curve), wavelengths around this critical wavelength are amplified, thus pushing the limit of how thin layers can safely be detected in the data. The resolution improvement is illustrated by the difference between the spectral amplitudes of the original and restored signals (orange and magenta curves in Figure 2a, respectively). Whereas the P_{signal} and P_{noise} curves intersect at $\lambda \approx 11$ mm for the original data, the signal part of the enhanced data spectrum intersect P_{noise} at $\lambda \approx 7$ mm.

A preliminary annual layer count illustrates the usefulness of the method. Using all the available CFA series, the annual layers have been identified. These layers are marked by grey, vertical bars in Figure 2c. The open grey bars indicate features that are possible annual layers, but that are less clearly identifiable. The restored signals support these uncertain annual layers as actual annual layers because peaks or clear "shoulders" are visible in all three restored data series at each of these depths. Also entirely new features appear in the restored series. The open magenta bars in Figure 2c mark annual layers present only in the restored series. It is not clear from the presented data series alone whether these features represent annual layers. A final decision will thus have to await cross checks with additional

data. By applying the method to the full length of the CFA profiles, and by applying the method to all species, it is hoped that the uncertainty of annual layer counting in the deeper parts of the NGRIP core can be significantly reduced due to the increased resolution.

An application of the method on a one meter section of $[Ca^{2+}]$ data from the Berkner Island ice core is illustrated in Figure 4. Due to a poor signal-to-noise ratio the method cannot safely restore much of the lost detail. This is due to the optimum filter $\widetilde{F}$ dropping below unity at higher wavelengths and decreasing more steeply than the inverse mixing filter $\widetilde{M}^{-1}$ rises. The resulting restoration filter $\widetilde{R}$ thus resembles the optimum filter $\widetilde{F}$ and the effect of the resolution enhancement is almost the same as using the optimum filter alone. In this case, little is gained from resolution enhancement point of view. However, from a data processing and interpretation point of view the produced signal is improved because of the included filtering. An important point is that the filtering is performed without manually choosing a low-pass filter cut-off frequency because the optimum filter in equation (7) automatically accommodates the signal-to-noise ratio of the data section in question.

The method will thus automatically improve the resolution as much as possible given the level of noise in the measurements and can therefore safely be applied to any data series as long as the (inverse) mixing filter is well determined. As the mixing filter reflects the combined mixing characteristics of the setup the mixing filter cannot be expected to remain unchanged when parts of the system are replaced, or when for example the melt speed is changed. Experiences obtained from both the NGRIP and Berkner Island measurements indicate that slow changes in the mixing characteristics due to wear take place with time but without affecting the results significantly. In contrast, changes in mixing characteristics due to replacement of tubing, columns, and flow cells or changes in melt speed are significant and the mixing filter must be modified to account for this. It is therefore advisable to integrate the mixing filter determination in the calibration operation so that a mixing filter is generated from every set of calibration measurements. By integrating the collection of calibrated blank-standard and standard-blank response curves in the data processing tools, most of the data needed for resolution enhancement can be gathered without much additional work. As an additional benefit, a comparison of the mixing characteristics from one measurement to the next gives a fast check on the system stability. The combination of system stability check and resolution enhancement means that the usefulness and reliability of the produced data can be significantly improved by the use of the presented method.

References

Alley, R. B., et al. (1997), Visual-stratigraphic dating of the GISP2 ice core: Basic, reproducibility, and application, *J. Geophys. Res.*, *102*(C12), 26,367–26,381.

Anklin, M., R. C. Bales, E. Mosley-Thompson, and K. Steffen (1998), Annual accumulation at two sites in Northwest Greenland during recent centuries, *Journal of Geophysical Research*, *103*(D22), 28,775–28,783.

Bigler, M. (2004), Hochauflösende Spurenstoffmessungen an polaren Eisbohrkernen: Glaziochemische und klimatische Prozessstudien, Ph.D. dissertation, University of Bern, Switzerland.

Bigler, M., D. Wagenbach, H. Fischer, J. Kipfstuhl, H. Miller, S. Sommer, and B. Stauffer (2002), Sulphate record from a northeast Greenland ice core over the last 1200 years based on continuous flow analysis, *Ann. Glaciol.*, *35*, 250–256.

Fuhrer, K., A. Neftel, M. Anklin, T. Staffelbach, and M. Legrand (1996), High-resolution ammonium ice core record covering a complete glacial-interglacial cycle, *J. Geophys. Res.*, *101*(D2), 4147–4164.

Hammer, C. U., H. B. Clausen, W. Dansgaard, N. Gundestrup, S. J. Johnsen, and N. Reeh (1978), Dating of Greenland ice cores by flow models, isotopes, volcanic debris, and continental dust, *J. Glaciol.*, *20*(82), 3–26.

Johnsen, S. J. (1977), Stable isotope homogenization of polar firn and ice, in *Proc. of Symp. on Isotopes and Impurities in Snow and Ice, I.U.G.G. XVI, General Assembly, Grenoble Aug./Sept., 1975*, pp. 210–219, IAHS-AISH Publ. 118, Washington D.C.

Johnsen, S. J., H. B. Clausen, K. M. Cuffey, G. Hoffmann, J. Schwander, and T. Creyts (2000), Diffusion of stable isotopes in polar firn and ice: The isotope effect in firn diffusion, in *Physics of Ice Core Records*, edited by T. Hondoh, pp. 121–140, Hokkaido University Press, Sapporo.

Legrand, M., and P. Mayewski (1997), Glaciochemistry of polar ice cores: A review, *Rev. Geophys.*, *35*(3), 219–243.

Littot, G. C., et al. (2002), Comparison of analytical methods used for measuring major ions in the EPICA Dome C (Antarctica) ice core, *Ann. Glaciol.*, *35*(1), 299–305.

McConnell, J. R., G. W. Lamorey, S. W. Lambert, and K. C. Taylor (2002), Continuous ice-core chemical analyses using inductively coupled plasma mass spectrometry, *Environmental Science and Technology*, *36*, 7–11.

Meese, D. A., A. J. Gow, R. B. Alley, G. A. Zielinski, P. M. Grootes, M. Ram, K. C. Taylor, P. A. Mayewski, and J. F. Bolzan (1997), The Greenland Ice Sheet Project 2 depth-age scale: Methods and results, *J. Geophys. Res.*, *102*(C12), 26,411–26,423.

North Greenland Ice Core Project members (2004), High-resolution record of Northern Hemisphere climate extending into the last interglacial period, *Nature*, *431*, 147–151.

Rasmussen, S. O., et al. (submitted to J. Geophys. Res.), A new Greenland ice core chronology for the last glacial termination.

Röthlisberger, R., M. Bigler, M. Hutterli, S. Sommer, B. Stauffer, H. Junghans, and D. Wagenbach (2000), Technique for continuous high-resolution analysis of trace substances in firn and ice cores, *Environ. Sci. Technol.*, *34*(2), 338–342.

Sigg, A. (1990), Wasserstoffperoxid-Messungen an Eisbohrkernen aus Grönland und der Antarktis und ihre atmosphärenchemische Bedeutung, Ph.D. dissertation, University of Bern, Switzerland.

Sigg, A., K. Fuhrer, M. Anklin, T. Staffelbach, and D. Zurmühle (1994), A continuous analysis technique for trace species in ice cores, *Environ. Sci. Technol.*, *28*, 204–210.

Sune Olander Rasmussen, Department of Geophysics, Niels Bohr Institute, University of Copenhagen, Juliane Maries Vej 30, DK-2100 Copenhagen, Denmark, olander@gfy.ku.dk.
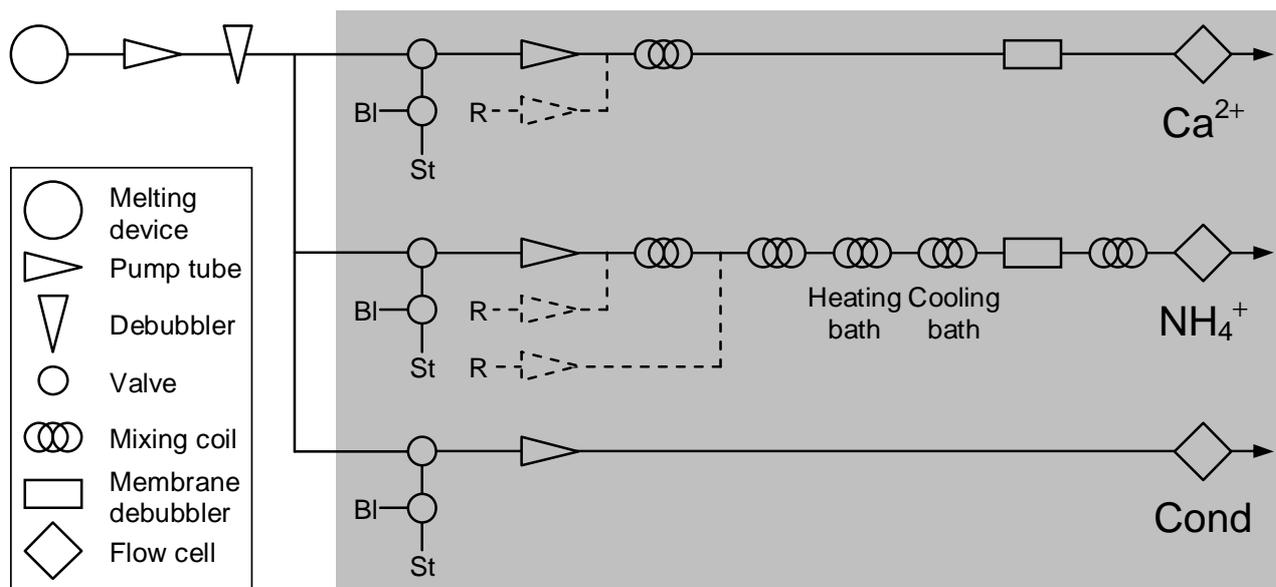
Figure 1. Simplified flow chart of the CFA setups for Ca^{2+}, NH_4^+ and electrolytical meltwater conductivity. Sample water from continuously melted ice is pumped to the warm lab, debubbled and split into substreams to feed the different analysis subsystems, where specific reagents (R) are added. Valves allow switching between sample, blank (Bl) or standard solution (St), which are used to establish baselines and calibrate the measurements. The total system comprise a set of different mixing volumes (tubing, debubbler, mixing coils, and flow cells as listed in the figure legend). However, in this work, only the part of the mixing that takes place within the grey shaded area is considered. Doted lines indicate the parts of the setup which do not contribute to the mixing.
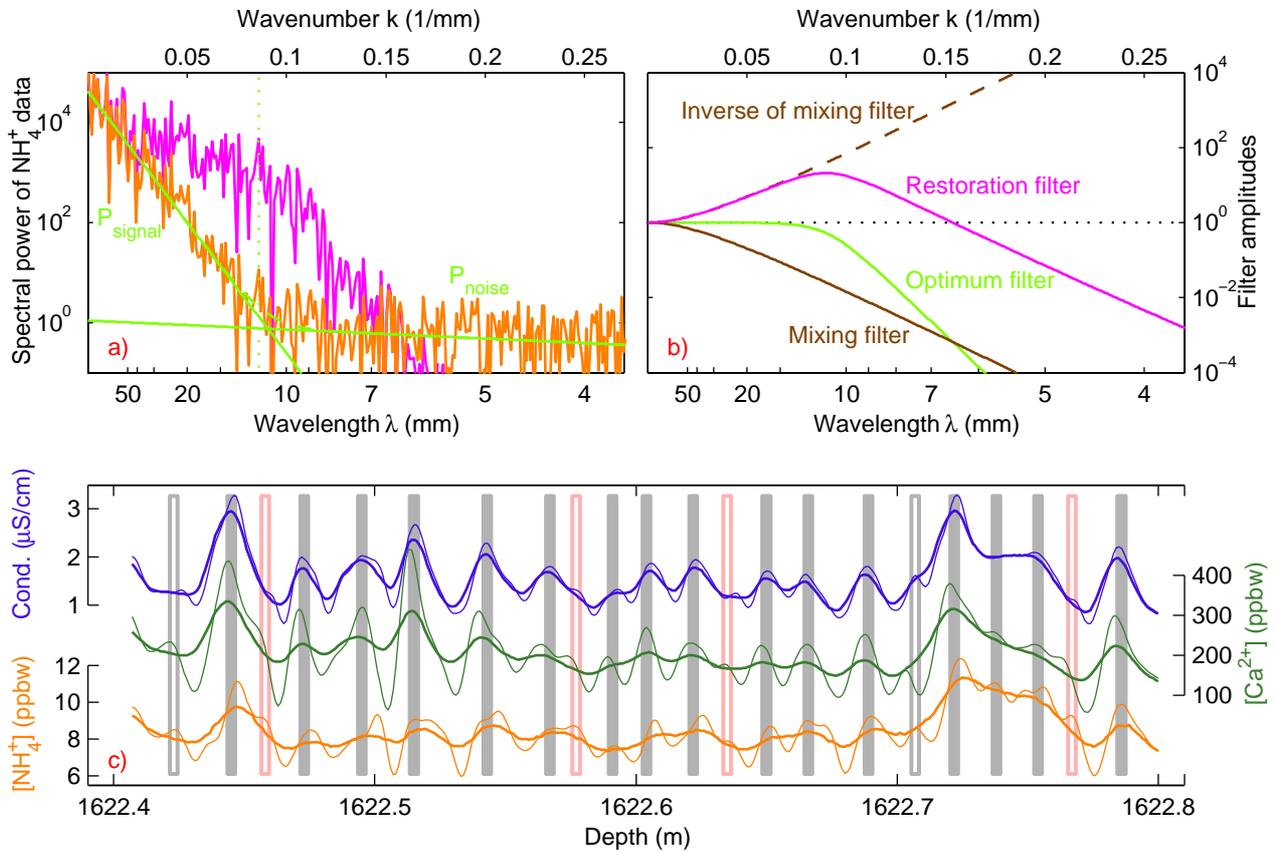
Figure 2. Data used to construct the deconvolution filters needed for signal restoration (a, b) and examples of the restored signals (c). The spectral power of a one meter NH_4^+ data section from about 1622 m depth (a, orange) has distinct signal and noise parts, P_{signal} and P_{noise}. This separation of the data spectral power into signal and noise parts defines the optimum filter (b, light green line) that allows restoration of the original signal without blowing up the noise. The strength of the mixing in the analysis system is estimated from the response curves (b, brown line). The inverted mixing filter (b, dashed brown line) is combined with the optimum filter (b, light green line), forming the restoration filter (b, magenta line). It is seen that the effect of the restoration is amplification of wavelengths down to 6–7 mm and that the maximum amplification is applied to wavelengths of about 11 mm. The spectral power of the restored signal is also shown (a, magenta line). For a data sequence from the Oldest Dryas, about 15 ka before present, the original data (c, heavy lines) and restored signals (c, thin lines) are shown together with suggested annual layers markings. See section 4 for additional details.
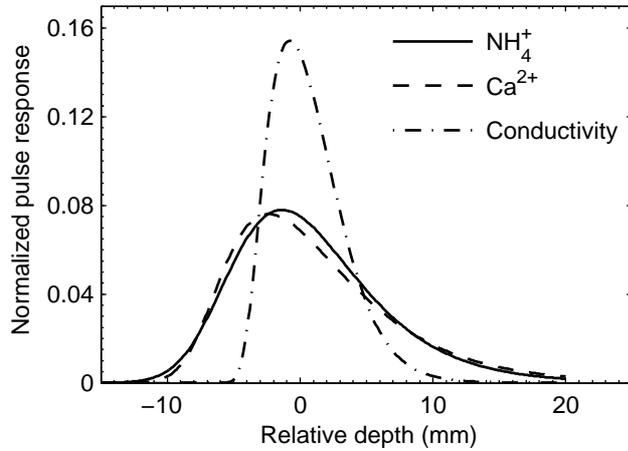
Figure 3. Response curves for the NGRIP NH_4^+, Ca^{2+}, and conductivity subsystems, showing the measured response to a delta function pulse at zero depth. For the NH_4^+ and Ca^{2+} subsystems, the pulse is spread out to become ~ 20 mm wide peaks, while the conductivity subsystem has a more narrow response curve corresponding to less mixing.
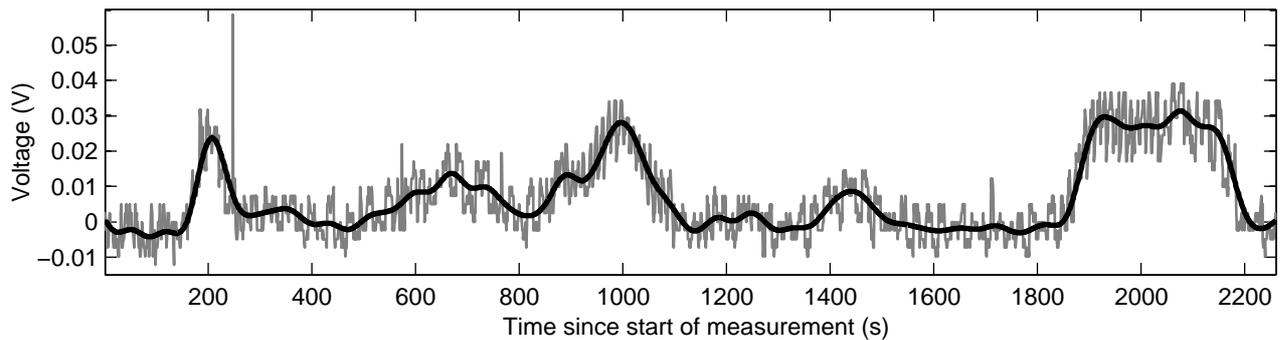

Figure 4. Example of the results of the resolution enhancement method (black curve) when applied to a 1 meter long raw $[Ca^{2+}]$ data sequence (grey curve) from the shallow part of the Berkner Island ice core. The presented sequence has a poor signal-to-noise ratio, but the method accounts for this via the optimum filter. Note how the spurious peak at 250 s (probably originating from an air bubble in the system) is removed by the filtering, easing the subsequent data processing.